The effect of the Caloris impact on the mantle dynamics and volcanism of Mercury

James H. Roberts and Oliver S. Barnouin, Johns Hopkins University Applied Physics Laboratory, 11100 Johns Hopkins Rd., Laurel, MD 20723-6099, United States, (James.Roberts@jhuapl.edu)

Introduction

MESSENGER has now imaged over 95% of the surface of Mercury, including the entirety of Caloris, the largest impact basin on Mercury [1]. These images reveal evidence for volcanic plains within and exterior to the basin that appear to be younger than the basin rim [2-4], and might be associated with the long-term aftermath of Caloris' formation. The broad influence of Caloris on the surface indicates that it might also affect heating of the deep mantle and thereby, the core. Here we investigate possible links between the Caloris impact on Mercury and volcanism within and surrounding the basin.

While the apparent age difference between the rim and plains [3-4] indicates that the plains materials cannot be impact melts, the thermal impulse from such an impact can alter the underlying mantle dynamics, producing volcanism late on. We use standard methods of impact scalings [5-8] and a finite element model of thermochemical convection in a spherical shell [9-11] to explore the melt production, and geodynamic evolution in the Mercurian mantle as a result of the Caloris impact.

Thermochemical Evolution

Figure 1 shows snapshots of the temperature, composition, and instantaneous melt fraction in the mantle within 30 ° of the impact site immediately before (a-c) and after the formation of Caloris by a projectile striking at 48 km/s (d-f), 24 km/s (g-i) and 12 km/s (j-l). Here, $Ra = 8.4 \times 10^6$, $B = 0.256$. Composition is shown in percent and varies between 0 for pristine mantle and 100 for the last remaining solid component (i.e. pure fortserite). The scale is saturated at a relatively low threshold (0.5%) to better show the boundary of incipient melting. Prior to the impact, only small amounts of melting occur in the convective upwellings. This melting occurs beneath the relatively thick stagnant lid where the temperature is the hottest. A significant fraction of the lower mantle of Mercury may be melted and mixed prior to any impact, simply due to the ambient mantle temperature and radioactive heating. The cooler stagnant lid is essentially unmelted prior to impact heating.

While the total energy delivered by the impactor is similar in all cases, the distribution of this energy depends on velocity. While all three projectiles produce a large amount of melt in the vicinity of the impact site,
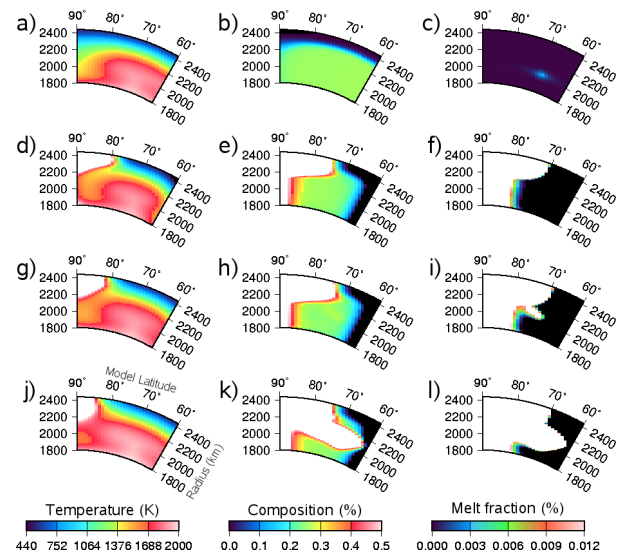

Figure 1: Temperature (left), composition (middle), and instantaneous melt production (right) in the Mercurian mantle within 30° of the impact site. immediately before (top row), and after a Caloris-forming impact at 48 km/s (second row), 24 km/s (third row) and 12 km/s (bottom row). All models are 2D axisymmetric and have $Ra = 8.4 \times 10^6$, $B = 0.255$, $E = 136$ kJ/mol, $V = 7.7$ cm^3/mol.

the broader distribution of heating in the slower impacts results in production of melt further away. In the case of the slowest projectile (12 km/s), significant melting occurs in the upwellings adjacent to the impact site.

The effect of the impact velocity on the distribution of melt can be illustrated by looking at the total melt fraction in a column, as shown in Figure 2. In each case the vast majority of melting occurs within 5° of the impact site. However, the 12 km/s projectile can also generate melting in the next upwelling over, thus producing a total column melt fraction of few percent at up to 20° from the impact site. The total amount of melting, however, is relatively insensitive to the velocity for a given impact energy, as shown in Figure 3. Prior to impact there is a significant amount of melting in convective upwellings where the plume temperature exceeds the solidus. The sharp rise in melt is due to the impact, the subsequent increase is due to upwelling material undergoing decompression melting. Similar total amounts of melt produc-
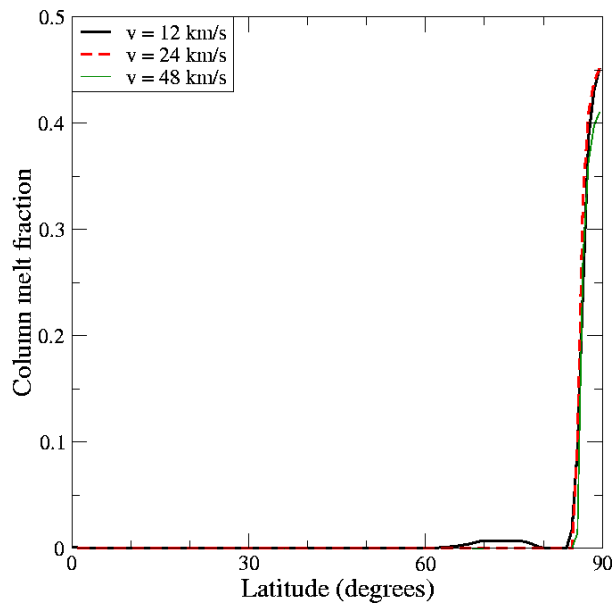
2

Figure 2: Total time-integrated column melt fraction vs. latitude immediately after formation of Caloris for the three impact velocities used for the models in Fig. 1.

Figure 3: Evolution of the total melt production over time for the models in Fig. 1.

tion ($\sim 0.25\%$ of the mantle) are obtained in all cases.

Younger volcanism

These results suggest that a single impact may produce multiple episodes of volcanism. The shock heating distribution from larger projectiles penetrates into convective upwellings up to 800 km away; beyond the basin rim. This promotes melt production in these upwellings, beneath a relatively thick stagnant lid. The associated melt is thus produced at depth and may be erupted to the surface much later than the direct impact melts. This is consistent with the relatively young age of the exterior plains [2-4]. We also find that impacts may sample different regions of the mantle. Direct impact melts are primarily in the near surface, while exterior melting is located in deeper mantle plume heads. Volcanic plains may therefore reveal pre-existing compositional stratification of the crust and mantle [2,12]. An additional interesting implication is that Impact melting may actually suppress volcanism at later times by prematurely using up the more easily melted components.

Effect on the core

We note that an impact capable of forming Caloris cannot significantly heat the core and should not affect the dy-
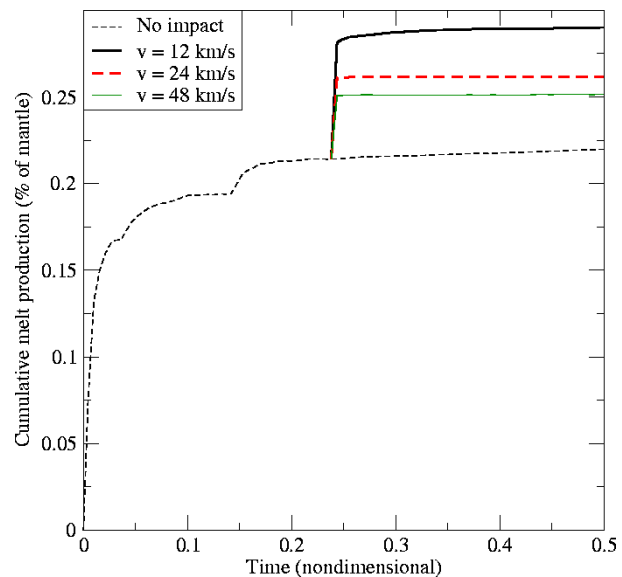
namo. This is consistent with observations of a present-day global magnetic field at Mercury [13]. The shock heating decays relatively quickly away from the impact site, due to the high expected impact velocity at Mercury (42.5 km/s [14]), and thus the small size of the projectile. We note, however, that the heating from a slow vertical impact could be mimicked by a fast oblique impact. Furthermore, while the median impact velocity at Mercury is high [14], the distribution is broad and some slower impacts are expected.

References

[1] Murchie, S.L. et al. (2008) *Science* 321, 73-76. [2] Denevi, B.W. et al. (2009) *Science* 324, 613-618. [3] Strom, R.G. (2008) et al. *Science* 321, 79-81. [4] Fassett, C.I. et al. (2009) *EPSL* 285, 297-308. [5] Melosh, H.J. (1989) *Impact Cratering*, Oxford Univ. Press. [6] Holsapple, K.A. (1993) *AREPS* 21, 333-373. [7] Pierazzo, E. et al. (1997) *Icarus* 127, 408-423. [8] Watters, W. A. et al. (2009) *JGR* 114, E02001. [9] Roberts, J.H. and S. Zhong (2004) *JGR* 109, E03009. [10] McNamara, A.K. and S. Zhong (2004) *JGR* 109, B07402. [11] Roberts, J.H. and O.S. Barnouin (2011) *JGR*, in revision. [12] Ernst, C.M. et al. (2010) *Icarus* 209, 210-223. [13] Anderson, B.J. et al. (2008) *Science* 321, 82-85. [14] Le Feuvre, M. and M. A. Wieczorek. (2008) *Icarus* 197, 391-206.